SLAC – PUB – 3835
September 1986
(T)

DISCRETIZED LIGHT–CONE QUANTIZATION: THE MASSLESS AND THE MASSIVE SCHWINGER MODEL*

THOMAS ELLER AND HANS-CHRISTIAN PAULI

Max-Planck-Institut für Kernphysik, D-6900 Heidelberg 1, Germany

and

STANLEY J. BRODSKY

Stanford Linear Accelerator Center
Stanford University, Stanford, California, 94305

ABSTRACT

The method of Discretized Light Cone Quantization (DLCQ), recently proposed for obtaining non-perturbative solutions to field theories, is applied to quantum-electrodynamics in one space dimension (QED_2). The spectrum of invariant masses and the eigenfunctions of the light-cone Hamiltonian are calculated; *i.e.*, the bound state problem is solved for all values of the coupling constant. For very strong coupling (Schwinger model proper) DLCQ reproduces one-to-one the known exact solutions. For non-vanishing fermion mass (massive Schwinger model) the results of DLCQ agree with earlier work and in particular with a lattice gauge calculation.

Submitted to *Physical Review D*

* Work supported in part by the Department of Energy, contract DE-AC03-76SF00515, by the National Science Foundation, Grant PHY82-17853, and supplemented by funds from the National Aeronautics and Space Administration.

1. INTRODUCTION

One of the most important tasks in particle physics is to calculate the spectrum of states in relativistic field theory, particularly gauge theory. In hadron physics it is critical to determine not just the spectrum of color singlet states in quantum chromodynamics, but also the quark and gluon composition of the hadron wavefunctions. Semiquantitative results for the low lying spectrum have been obtained in the lattice version of QCD, but reliable calculations of hadron wavefunctions are computationally arduous, and only very approximate measures have been obtained. The lattice calculations are particularly hampered by the difficulties associated with dynamical fermions. Important constraints on moments of wavefunctions have been obtained using the QCD sum rule technique, but the numerical reliability of this method is difficult to ascertain.

In this paper we continue our development of the discretized light cone quantization method (DLCQ)[1,2] and give the first application to gauge theory. By quantizing at equal time on the light cone in $A^+ = 0$ gauge[3-11] a gauge theory can be reduced to an eigenvalue problem for the light cone Hamiltonian:

$$H_{LC}\Psi = M^2\Psi \quad .$$

Taking periodic boundary conditions in the x^- direction,[1,9,10] requires that the total light cone momentum $P^+ = 2\pi K/L$. Since each constituent momentum $k^+ = 2\pi n/L$ must be positive, this restricts the Fock state basis for Ψ to finite dimensional representations (corresponding to the number of partitions of the integer K as a sum of positive integers n). The invariant mass does not depend[1,9] on the period L.

This method has a number of important computational advantages:

(1) The relativistic spectrum emerges as the set of eigenvalues

$$M^2 = M_1^2, M_2^2, ...$$

of a finite, Hermitian, relatively sparse matrix — the light cone Hamiltonian.

(2) The wavefunctions are the corresponding eigensolutions of the H_{LC}. In momentum space each component $\psi_n(x, k_T, \lambda)$ corresponds to a finite number of quarks and gluons as a function of the light cone momenta and helicities. Given the ψ_n one can compute hadronic static quantities, current matrix elements, structure functions, and distribution amplitudes, thus allowing empirical tests of the full structure of the theory.

(3) Since one works in momentum space there is no problem with fermion doubling or other special complications involving fermion variables.

(4) Since the light cone gauge is physical there are no negative metric components in either Abelian or non-Abelian theories.

(5) The approach to the continuum theory is set by magnitude of the harmonic resolution K not by the periodicity scale L (which is arbitrary). As K becomes large the momentum space structure is resolved at a finer grid of rational points $k^+ \sim n/K$. Unlike the spacetime lattice there is no matching condition between the wavefunction size and lattice size in DLCQ.

The Schwinger model[12–16] (massless QED in one space and one time dimensions) and its massive fermion counterpart (QED_2)[3–27] have served as showcases for important aspects of field theory such as confinement or bosonization.[28–30] In this paper these theories will serve as important first tests of the application of

DLCQ to gauge theory. Because of the lack of transverse dimensions the quanta corresponding to photons or gluons do not appear. In the case of the Schwinger model the fermions are confined, and the theory is equivalent to a free theory of bosons[12] with physical mass $\tilde{m} = g/\sqrt{\pi}$. In DLCQ this spectrum emerges naturally if one takes care to properly include zero mode fermions; i.e. fermion states with zero energy and momentum components.[9] Remarkably, the exact spectrum is obtained as the solution for any value of the resolution K since in the Schwinger model the momentum distribution of the bound state wavefunction is flat in x.[24]

In the case of massive QED_2, the zero mode fermions do not appear, and we can solve for the spectrum and eigensolutions numerically at any coupling strength. The DLCQ method is straightforward and efficient; the results converge rapidly as K increases and agree rather well with previous results obtained numerically using the lattice or equal time quantization. We also give the structure function for the lowest mass solution and the probability for finding non-valence Fock components.

Thus at this point DLCQ appears to be a quantitative alternative to existing non-perturbative methods.[17–24] Applications to three-space one-time theories are much more difficult due to the gluon degrees of freedom, the transverse momenta, as well as color labels for the non-Abelian theories. An important and interesting application is to ordinary QED_4 which can be studied for arbitrary coupling constant in DLCQ. One can thus provide an important check on the range of validity of perturbative expansions for the lepton moments and the positronium Lamb shift or hyperfine splitting. Photon zero modes are irrelevant since they decouple from gauge invariant quantities such as the wavefunctions of neutral bound states.

The procedure of DLCQ and the present work can be briefly outlined. One starts with the Lagrangian density and calculates canonically the energy-momentum operators P^ν in terms of the independent fields. The independent fields are quantized at equal light cone time and identified with the free field solutions; *i.e.* , with the most general superposition of plane waves created and destructed by anticommuting operators. In this way one expresses energy-momentum as operators which act in Fock space (see section 2). Imposing periodic boundary conditions, the plane wave momenta become discrete. Lorentz-invariance is violated by discretization but is retrieved at the end of the calculation in the continuum limit, $K \to \infty$, to be discussed more thoroughly in section 3. Discretization allows one to associate discrete (and for that matter finite dimensional) matrices with each of the operators P^ν. They can be diagonalized by standard numerical methods. For example, one generates eigenvalues of the invariant mass squared $M^2 = P^\nu P_\nu$ which for the Schwinger model agree one-to-one with the exact values (see section 4). The massive Schwinger model and its numerical solutions are discussed in section 5. They agree rather well with previous work.[26,24] The mass spectrum and the structure function of the lowest mass eigenstate are discussed in section 6. Conclusions and prognosis for future work in physical gauge theories are discussed in section 7.

2. THE FOCK SPACE OPERATORS FOR QED$_2$

Quantum Electrodynamics (QED) describes massive fermions ψ interacting with massless photons A^μ as specified by the Lagrangian density

$$\mathcal{L} = \frac{i}{2}\left(\overline{\psi}\gamma^\mu\partial_\mu - \partial_\mu\overline{\psi}\gamma^\mu\right)\psi - m\overline{\psi}\psi - \frac{1}{4}F^{\mu\nu}F_{\mu\nu} - g\overline{\psi}\gamma^\mu\psi A_\mu \quad , \tag{2.1}$$

where $F^{\mu\nu} \equiv \partial^\mu A^\nu - \partial^\nu A^\mu$ is the usual electro-magnetic field tensor. The canonical formalism for one space and one time dimension using light cone coordinates $x^\pm = x^0 \pm x^1$ is well known.[1-8] For notational reasons we shall give a short summary here. The metric tensor $g^{\mu\nu}$ for the light cone coordinates[1] has the form $(g^{++} = g^{--} = 0,\ g^{+-} = g^{-+} = 2)$. One must distinguish upper and lower indices; for example, time derivatives $\partial^- = 2\partial_+ \equiv 2\partial/\partial x^+$ and space derivatives $\partial^+ = 2\partial_- \equiv 2\partial/\partial x^-$ should not be confused. The Dirac matrix algebra, *i.e.* $\gamma^+\gamma^+ = \gamma^-\gamma^- = 0$ and $\gamma^+\gamma^- + \gamma^-\gamma^+ = 4$, is useful for defining projection operators[1,6] $\Lambda^{(\pm)} \equiv \frac{1}{4}\gamma^\mp\gamma^\pm$ and projected spinors $\psi_\pm \equiv \Lambda^{(\pm)}\psi$. In light cone gauge[3] $A^+ = 0$, Maxwell's equations $\partial_\nu F^{\nu\mu} = g\, j^\mu$ reduce to only one equation $-\partial_-\partial^+ A^- = g j^+$ where the light cone fermion density is $j^+ \equiv \overline{\psi}\gamma^+\psi = 2\psi_+^\dagger\psi_+$. The vector potential is determined in this gauge by the fermion field ψ_+, *i.e.*

$$A^- = 4g\frac{1}{(i\partial^+)^2}(\psi_+^\dagger\psi_+) \quad . \tag{2.2}$$

In 1+1 dimensions the transverse directions are absent and the photons do not appear as dynamical degrees of freedom. The inverse derivatives $(i\partial^+)^{-1}$ and $(i\partial^+)^{-2}$ are used as a convenient notation. In practice, they involve Green's

functions (see appendix A); for example

$$\frac{1}{(i\partial^+)^2}\phi(x^-) = -\frac{1}{8}\int_{-\infty}^{\infty} dy\,|x^- - y|\,\phi(y) \quad + Fx^- + C\ .$$

The c-numbers F and C represent background fields which lead to interesting phenomena as discussed by Coleman et al.[18,19] In the present work they are set to zero because of boundary conditions.

The Dirac equation $(i\gamma^\mu\partial_\mu - m)\,\psi = g\gamma^\mu A_\mu\psi$ is reduced to two coupled equations $i\partial^-\psi_+ = m\,\gamma^0\psi_- + gA^-\psi_+$ and $i\partial^+\psi_- = m\,\gamma^0\psi_+$. One notes that ψ_- is determined by ψ_+, *i.e.* $\psi_- = m\,\gamma^0\,(i\partial^+)^{-1}\psi_+$ and that the light cone time derivative of ψ_+, *i.e.*

$$i\partial^-\psi_+ = 4g^2\psi_+\frac{1}{(i\partial^+)^2}(\psi_+^\dagger\psi_+) + m^2\,\frac{1}{(i\partial^+)}\,\psi_+ \quad , \tag{2.3}$$

is a functional of ψ_+ alone. The only independent field is thus ψ_+, and as such is subject to quantization

$$\left\{\psi_+(x),\ \psi_+^\dagger(y)\right\}_{x^+=y^+} = \Lambda^{(+)}\,\delta(x^- - y^-) \tag{2.4}$$

at equal light cone time.[1-8]

The Lagrangian Eq. (2.1) gives rise to conserved currents. Only two of them are considered in this work, namely the fermion current $j^\nu = \overline{\psi}\gamma^\nu\psi$ and the energy-momentum tensor $\mathcal{T}^{\mu\nu} = \frac{i}{2}\left(\overline{\psi}\gamma^\mu\partial^\nu\psi - \partial^\nu\overline{\psi}\gamma^\mu\psi\right) + F^{\lambda\mu}\partial^\nu A_\lambda - g^{\mu\nu}\mathcal{L}$. The conserved currents lead to conserved charges, *i.e.* $Q = \frac{1}{2}\int dx^-\ j^+(x^-, x_0^+)$ and $P^\nu = \frac{1}{2}\int dx^-\ \mathcal{T}^{+\nu}(x^-, x_0^+)$. The charge Q, the light cone momentum P^+ and the light cone Hamiltonian P^- form a set of mutually commuting operators.[6]

Consequently, they can be diagonalized simultaneously, which is equivalent to solving the equations of motion. Using Eqs. (2.2) and (2.3) one obtains after partial integration

$$Q = \int dx^- \psi_+^\dagger \psi_+ \,, \qquad P^+ = \int dx^- \psi_+^\dagger i\partial^+ \psi_+ \quad \text{and} \tag{2.5}$$

$$P^- = m^2 \int dx^- \psi_+^\dagger \frac{1}{(i\partial^+)} \psi_+ + 2g^2 \int dx^- \psi_+^\dagger \psi_+ \frac{1}{(i\partial^+)^2} (\psi_+^\dagger \psi_+) \quad . \tag{2.6}$$

The explicit construction of these quantities as operators which act in Fock space is the aim of this section.

The independent spinor field $\psi_+ = \psi_+(x^-, x_0^+)$ can be chosen freely at an arbitrary light cone time x_0^+ provided one satisfies the anticommutation relation; for example, it can be chosen as the most general solution of the free Dirac equation with vanishing mass, *i.e.* of $i\partial^- \psi_+ = 0$. Obviously, the solution cannot depend on the light cone time, thus

$$\psi_+(x^-, x^+) = u \, \frac{1}{\sqrt{2L}} \left(B_0 + D_0^\dagger + \sum_{n=1}^{\Lambda} b_n \, e^{-in\xi} + d_n^\dagger \, e^{+in\xi} \right) \tag{2.7}$$

$$\text{with} \quad \xi = \pi \frac{x^-}{L} \quad .$$

We have imposed periodic boundary conditions in x^-, see also refs.9 and 10. The momenta $k^+ = 2k_- = n\frac{2\pi}{L}$ $(n = 0, 1, \ldots, \Lambda)$ become discrete, a condition which is relaxed in the *continuum limit* as discussed below.

The spinor u is fixed by the projection $u = \Lambda^{(+)} u$ and by the normalization $u^\dagger u = 1$. The creation and destruction operators obey the familiar anticommu-

tation relations. They vanish, except for

$$\left\{b_n, b_m^\dagger\right\} = \left\{d_n, d_m^\dagger\right\} = \delta_{n,m} \ , \quad \text{but} \quad \left\{B_0, B_0^\dagger\right\} = \left\{D_0, D_0^\dagger\right\} = \frac{1}{2} \ . \tag{2.8}$$

By explicit calculation one can verify the field commutation relations, Eq. (2.4).

Because of Eq. (2.7) the operators P^+ and P^- depend on the period L. This dependence turns out to be explicit, *i.e.*

$$P^+ = \frac{2\pi}{L} K \quad \text{and} \quad P^- = \frac{L}{2\pi} H \ . \tag{2.9}$$

The invariant mass squared becomes $M^2 = P^+P^- = K\,H$, *i.e. independent of* L.[1,9]

Upon inspection of Eq. (2.6) one can define

$$H = m^2\, H_0 + \frac{g^2}{\pi} V \ . \tag{2.10}$$

In $1+1$ dimensions the coupling constant has the dimension of a mass.[12] Thus all operators under consideration, *i.e.* the charge Q, the harmonic resolution K, the inertia H_0 and the interaction V are dimensionless. Their evaluation is enormously simplified by introducing the dimensionless matrix elements

$$\{n|m\} \equiv \frac{1}{2\pi} \int_{-\pi}^{\pi} d\xi \; e^{in\xi} \, \frac{1}{i\partial_\xi} \, e^{im\xi} \ , \quad [n|m] \equiv \frac{1}{2\pi} \int_{-\pi}^{\pi} d\xi \; e^{in\xi} \, \frac{1}{(i\partial_\xi)^2} \, e^{im\xi} \ . \tag{2.11}$$

As shown in the appendix they are well-defined

$$\begin{aligned} \{n|m\} &= \frac{1}{n}\delta_{n+m,0}, \quad \{n|0\} = \{0|m\} = 0, \quad \{0|0\} = 0 \ , \qquad \text{and} \\ [n|m] &= \frac{1}{n^2}\delta_{n+m,0}, \quad [n|0] = [0|m] = 0, \qquad [0|0] = -\kappa^2 \ , \ \kappa \to \infty \ . \end{aligned} \tag{2.12}$$

It is then straightforward to show that

$$K = \sum_{n=1}^{\Lambda} n \left(b_n^\dagger b_n + d_n^\dagger d_n \right) \qquad \text{and} \quad H_0 = \sum_{n=1}^{\Lambda} \frac{1}{n} \left(b_n^\dagger b_n + d_n^\dagger d_n \right) . \tag{2.13}$$

Both are diagonal and independent of the zero-momentum fermions B_0 and D_0, as opposed to the charge which is off-diagonal in the latter. However, Q can be diagonalized by a Bogoliubov transform. By introducing quasi-fermions[9]

$$b_0 = B_0 + D_0^\dagger \qquad \text{and} \quad d_0^\dagger = B_0 - D_0^\dagger \quad , \tag{2.14}$$

with anticommutation relations $\left\{ b_0, b_0^\dagger \right\} = \left\{ d_0, d_0^\dagger \right\} = 1$ according to Eq. (2.8), the charge becomes

$$Q = \sum_{n=0}^{\Lambda} \left(b_n^\dagger b_n - d_n^\dagger d_n \right) \equiv b_0^\dagger b_0 + \sum_{n=1}^{\Lambda} \left(b_n^\dagger b_n - d_n^\dagger d_n \right) \quad . \tag{2.15}$$

Here and in the following we can formally set $d_0 \equiv 0$, since ψ_+ and hence Q does not depend on it.

The interaction V

$$\begin{aligned} V = \frac{1}{2} \sum_{k,l,m,n=0}^{\Lambda} & \left(b_k^\dagger d_l^\dagger b_m^\dagger d_n^\dagger + d_n b_m d_l b_k \right) [k+l|m+n] + \\ & \left(b_k^\dagger b_m d_l^\dagger d_n + b_m b_k^\dagger d_n d_l^\dagger \right) [k+l|-m-n] + \\ & \left(b_k^\dagger b_m b_l^\dagger b_n + d_m d_k^\dagger d_n d_l^\dagger + b_k^\dagger b_m d_n d_l^\dagger + b_k^\dagger b_m d_n d_l^\dagger \right) [k-m|l-n] + \\ & \left(d_k^\dagger b_l^\dagger b_m^\dagger b_n + b_k d_l d_m d_n^\dagger + b_k^\dagger d_m^\dagger d_n d_l^\dagger + d_l d_n^\dagger d_m b_k \right) [k+m|l-n] + \\ & \left(d_k b_m b_n^\dagger b_l + b_l^\dagger b_n b_m^\dagger d_k^\dagger + d_k b_n^\dagger b_l b_m + b_k^\dagger d_n d_l^\dagger d_m^\dagger \right) [k+m|l-n] \end{aligned} \tag{2.16}$$

is divided into three parts

$$V = V_Q + V_N + V_C \quad . \tag{2.17}$$

The *charge dependent part* V_Q contains *all* of the dependence on the matrix

element [0|0], *i.e.*

$$V_Q = \frac{1}{2}[0|0] \sum_{k,n=0}^{\Lambda} \left(b_k^\dagger b_k b_n^\dagger b_n + d_k d_k^\dagger d_n d_n^\dagger + b_k^\dagger b_k d_n d_n^\dagger + b_k^\dagger b_k d_n d_n^\dagger \right) \quad ,$$

and can be written as $V_Q = \frac{1}{2}[0|0]\ (Q+\Lambda)^2$. The cut-off Λ is a *c*-number and V_Q becomes finally

$$V_Q = \frac{1}{2} Q [0|0]\, (Q + 2\Lambda) \ . \tag{2.18}$$

Since V_Q contains all dependence on [0|0], by definition one has [0|0] = 0 in the remainder, *i.e.* in V_N and V_C to be defined. The *normal ordered part* V_N of the interaction V becomes

$$\begin{aligned} V_N = \sum_{k,l,m,n=0} & \left(b_k^\dagger b_l^\dagger b_m b_n + d_k^\dagger d_l^\dagger d_m d_n \right) \ [k-n|l-m]/2 \ + \\ & b_k^\dagger b_l d_m^\dagger d_n \ ([k+m|-l-n] - [k-l|m-n]) \ + \\ & \left(b_k^\dagger d_l^\dagger d_m^\dagger d_n + d_n^\dagger d_m d_l b_k \right) \ [k+m|l-n] \ + \\ & \left(d_k^\dagger b_l^\dagger b_m^\dagger b_n + b_n^\dagger b_m b_l d_k \right) \ [k+m|l-n] \quad . \end{aligned} \tag{2.19}$$

The sum of all pairwise *contractions* of V is denoted by V_C . It turns out to be diagonal due to the selection rules in the matrix elements, Eq. (2.12) , *i.e.*

$$V_C = \sum_{n=1}^{\Lambda} I_n \left(b_n^\dagger b_n + d_n^\dagger d_n \right) + \left\{ b_0, b_0^\dagger \right\} \sum_{n=1}^{\Lambda} \frac{1}{2n^2} \left(b_n^\dagger b_n - d_n^\dagger d_n \right) \quad . \tag{2.20}$$

To clarify the origin of the second term, the anticommutator $\left\{ b_0, b_0^\dagger \right\} = 1$ has been written out explicitly. The *self-induced inertias*[1]

$$I_n \equiv \frac{1}{2} \sum_{m=1}^{\Lambda} \left([n-m|m-n] - [n+m|-n-m] \right) = -\frac{1}{2n^2} + \sum_{m=1}^{n} \frac{1}{m^2} \tag{2.21}$$

take the value

$$I_n = \frac{1}{2}\,,\ \frac{9}{8}\,,\ \frac{47}{36}\,,\ \frac{401}{288}\,,\ \ldots\,,\ \frac{\pi^2}{6} \quad \text{for} \quad n = 1,2,3,4,\ldots,\infty \tag{2.22}$$

in the limit $\Lambda \to \infty$.

At first sight it appears as if the light-cone Hamiltonian, specifically the last term in V_C, Eq. (2.20), is not invariant under charge conjugation when the zero momentum fermion operator is included. The charge conjugation operator C is defined such that $CB_0C^{-1} = D_0$ and $CD_0C^{-1} = B_0$. According to Eq. (2.14) the quasi-particles transform therefore like $Cb_0C^{-1} = b_0^\dagger$. In the interaction V_N, Eq. (2.19), the quasiparticles appear in exactly three combinations, *i.e.* linear in b_0, in $b_0^\dagger$ and in $b_0^\dagger b_0$. If one picks up the last combination and adds it to the second half of Eq. (2.20) , one gets

$$\left(\frac{1}{2} - b_0^\dagger b_0\right) \sum_{n=1}^{\Lambda} \frac{1}{n^2} \left(b_n^\dagger b_n - d_n^\dagger d_n\right) \quad .$$

This expression, as well as the remaining terms in the Hamiltonian is charge conjugation invariant.

As mentioned, the initial field $\psi_+ = \psi_+(x^-, x_0^+)$ appearing in Eqs. (2.5) and (2.6) is arbitrary. As an alternative, it can be chosen as a solution of the free *massive* Dirac equation $i\partial^-\psi_+ = m_F\,\gamma^0\psi_-$ and $i\partial^+\psi_- = m_F\,\gamma^0\psi_+$, *i.e.* of $-\partial^-\partial^+\psi_+ = m_F^2\,\psi_+$ with an *arbitrary* fermion mass m_F. Since m_F is non-zero, the quasi-fermion cannot be a partial solution as in Eq. (2.7), but the most general solution taken at $x_0^+ = 0$ is independent of m_F,[1] *i.e.*

$$\psi_+(x^-, x_0^+) = u\,\frac{1}{\sqrt{2L}} \sum_{n=1}^{\Lambda} b_n\, e^{-in\xi} + d_n^\dagger\, e^{+in\xi} \text{ with } \xi = \pi\frac{x^-}{L} \quad . \tag{2.23}$$

In order to get the Fock space operators for this alternative basis, the *massive*

representation, one can set formally $b_0 \equiv 0$ in Eqs. (2.15), (2.19) and (2.20); in particular, the commutator term in Eq. (2.20) is omitted.

Finally, one can verify by explicit calculation that the operators Q and P^ν commute also as Fock space operators, as they should,[6] irrespective of whether one includes the zero-momentum fermions or not.

3. DISCUSSION OF THE PROCEDURE

As in other field theories, QED_2 contains an *arbitrary scale.* This becomes particularly clear in the notation of Eq. (2.10) , *i.e.* $H = m^2 H_0 + \frac{g^2}{\pi} V$. If one scales both the fermion mass and the coupling constant by some number C, the Hamiltonian and thus the whole mass spectrum scales by the same amount, *i.e.*

$$m \to m' = Cm, \qquad g \to g' = Cg, \qquad \text{thus } M_i \to M_i' = CM_i \ .$$

Therefore, apart from a scale, the spectrum cannot depend on m or g separately, but only on the dimensionless ratio g/m. It is thus natural to use the parameterization

$$\frac{g}{\sqrt{\pi}} \equiv \tilde{m}\lambda \qquad \text{and} \quad m \equiv \tilde{m}\sqrt{1-\lambda^2} \quad , \text{thus } \lambda = \sqrt{\frac{1}{1+\pi\,(m/g)^2}} \tag{3.1}$$

which maps the entire range of both m and g onto the finite interval $0 \leq \lambda \leq 1$. The numerical value of $\tilde{m}$ is irrelevant. The final expression for the invariant mass squared is thus

$$M^2 = \tilde{m}^2 \left\{ (1-\lambda^2) K H_0 + \lambda^2 K V \right\} \ . \tag{3.2}$$

If not mentioned otherwise the invariant mass eigenvalues will be given in units where $\tilde{m}$ takes the numerical value 1. In sec. 6 we will choose $\tilde{m}$ to *renormalize*

the spectrum such that the lowest mass eigenvalue $M = 1$, independent of the interaction strength λ.

The operators of charge, momentum and energy derived in sec. 2 are operators which act in Fock space, *i.e.* in the representation which diagonalizes the number operators $b_n^\dagger b_n$ and $d_n^\dagger d_n$. Each Fock state $|\Phi_i\rangle$ is characterized by the single particle discretized momenta n which are occupied by a particle or an anti-particle; for instance

$$|\Phi_i\rangle = |n_1, n_2, \ldots, n_N; \bar{n}_1, \bar{n}_2, \ldots, \bar{n}_{\bar{N}}\rangle \equiv b_1^\dagger, b_2^\dagger, \ldots b_N^\dagger d_1^\dagger d_2^\dagger \ldots d_{\bar{N}}^\dagger |v\rangle \quad , \qquad (3.3)$$

where $|v\rangle$ denotes the vacuum. The set of all possible Fock states represent the Hilbert space in which one calculates the matrix elements of the three operators under consideration, *i.e.* $\langle i| Q |j\rangle$, $\langle i| K |j\rangle$ and $\langle i| H |j\rangle$.

The charge operator Q is diagonal in the Fock space representation (see Eq. (2.5)). As is well known, QED_2 does not allow for free charges.[18,19] In the present approach this fact manifests itself in the operator V_Q (Eq. (2.18)), which diverges for all non-zero charges. Since this divergence cannot be removed by renormalization, QED_2 must be confined to the charge zero sector. The momentum operator $P^+ = K\frac{2\pi}{L}$ is also diagonal (see Eq. (2.5)). Many Fock states can have the same eigenvalue K and $Q = 0$, but their number $N_{dim} \equiv N_{dim}(K)$ is *strictly finite* due both to the fact that n is positive or zero and due to the exclusion principle.

The light cone energy $P^- = H\frac{L}{2\pi}$ is not diagonal for finite interaction λ. If one orders all possible Fock states according to the eigenvalue of K, it becomes block diagonal because P^- commutes with both P^+ and Q, *i.e.* $\langle \Phi(K')| H |\Phi(K)\rangle = 0, \quad$ for $K' \neq K$. The dimension of each block matrix is finite and equal to

N_{dim}. Each block can then be diagonalized numerically. As a result of diagonalization one obtains the eigenvalues of the invariant mass squared $M^2 = KH$ together with the coefficient matrix C_j^i which represents the eigenstates

$$|M_i\rangle = \sum_{j=1}^{N_{dim}} C_i^j \, |\Phi_j\rangle \quad . \tag{3.4}$$

The Fock states for the four lowest values of K are displayed in Table 1 together with the corresponding blocks of the Hamiltonian. The table lists the elements of the invariant mass squared, split into the diagonal KH_0 and off diagonal KV terms according to Eq. (2.10). The finiteness, and in fact the relative smallness of the matrices, is an attractive feature of DLCQ. Unfortunately the dimension increases exponentially for large values of K, as shown in Table 2. In the computer codes the matrix dimension has been limited to $N_{dim} \leq 256$.

DLCQ imposes periodic boundary conditions and discretizes the (light cone) momenta $k^+ = 2\pi\frac{n}{L}$ or $P^+ = 2\pi\frac{K}{L}$. This violates Lorentz invariance but the continuum can be regained by a limiting procedure, *i.e.*

$$L \to \infty, \qquad K \to \infty, \qquad \text{but} \quad P^+ = 2\pi\frac{K}{L} \quad \text{finite} \quad , \tag{3.5}$$

and similarly for $k^+ = 2\pi n/L$. The *physical* spectrum $M_i(K)$ is thus obtained only in the *continuum limit* $K \to \infty$, and in the strict sense this limit cannot be reached. In practice, it can be approximated to arbitrary accuracy by studying the convergence of the mass spectrum $M(K)$ as it becomes sufficiently independent of K. But discretization has obvious advantages, not the least being the *denumerability of Fock states* and the representation of Fock space operators as strictly finite dimensional matrices. The spectrum is manifestly independent of

the two formal and redundant parameters, the cut-off in single particle momenta Λ and the period L. Last, but not least, as we discuss in the next sections, the *qualitative aspects* of the solutions show up at comparatively small value of the resolution[1] K.

4. THE STRONG LIMIT: THE SCHWINGER MODEL

The Schwinger model is defined as QED_2 with vanishing Lagrangian mass. As shown by Schwinger[12] this theory is equivalent to the theory of free massive neutral bosons: The boson fields A^ν obey

$$\left(\partial_\mu \partial^\mu + \tilde{m}^2\right) A^\nu = 0 \ , \quad \text{with mass} \quad \tilde{m} \equiv \frac{g}{\sqrt{\pi}} \quad . \tag{4.1}$$

According to Casher, Kogut and Susskind,[14] non-zero charge solutions *i.e.* free electrons cannot exist; they would acquire an infinite mass.

To make the comparison between the Schwinger model and the bosonized theory, it is convenient to cast Eq. (4.1) into a Lagrangian, quantize at equal light cone time and calculate energy and momentum in very much the same way as in ref.1 . The operators of invariant mass squared M^2 and of resolution K are then given by

$$M^2 = \tilde{m}^2 K \sum_{n=1}^{\Lambda} \frac{1}{n} a_n^\dagger a_n, \quad \text{and} \quad K = \sum_{n=1}^{\Lambda} n\, a_n^\dagger a_n, \tag{4.2}$$

respectively. The boson operators obey $[a_n, a_m^\dagger] = \delta_{n,m}$. In other words, the momentum and the energy of the Schwinger model are diagonal in the Boson representation, and one can readily evaluate the spectrum of invariant masses.

For small resolution they are given in Table 3 in units of $\widetilde{m}$, together with the corresponding boson Fock states. Their number for each K is identical with the number of fermion Fock states (see Table 1).

The Schwinger model mass spectrum is plotted in Fig. 1 as a function of the resolution. In the lowest state $\left|\widetilde{K}^1\right\rangle$ one boson takes all the momentum K and has invariant mass $M = 1$. In the next higher states the total momentum K is shared by two bosons. According to Eq. (4.2) one has

$$\left(M^2 - \frac{4}{1-(n/K_2)^2}\right)\left|\widetilde{K_2} - \widetilde{n}, \widetilde{K_2} + \widetilde{n}\right\rangle = 0 \quad \text{for} \quad n = 0, 1, \ldots, K_2 - 1, \quad (4.3)$$

where $K_2 \equiv K/2$. The state $\left|\widetilde{K_2}^2\right\rangle$ describes two bosons at rest relative to each other, with an invariant mass of precisely $M = 2$. The states with relative momenta $n \geq 1$ generate masses $M > 2$, *i.e.* a band spectrum corresponding to two bosons in relative motion. Similarly, states with $M = 3, 4 \ldots$ correspond to $3, 4 \ldots$ bosons at relative rest, each of them being at the head of a band of states in the continuum limit. The spectrum ends with a state $\left|\widetilde{1}^K\right\rangle$ of mass $M = K$ corresponding to a boson condensate of K bosons with momentum $n = 1$.

The *continuum limit* is now obvious. The lowest state is isolated and has an invariant mass $M = 1$. Above $M = 2$ follows a continuum of states corresponding to two or more bosons in relative motion.

Returning to Eq. (3.2) the Lagrangian mass m approaches zero in the strong coupling limit $\lambda \to 1$, and the invariant mass in the DLCQ approach satisfies the equation $M^2 = \widetilde{m}^2 KV$. Examples of the matrices KV are given in Table 1. In order to obtain the eigenvalues, these matrices must be diagonalized. For resolutions $K = 1$ and $K = 2$ this can be done analytically; the eigenvalues 1

and 4 agree precisely with the exact results in Table 3. For the higher resolutions diagonalization can be done numerically. *The numerical identity of all eigenvalues with the exact values of Eq.* (4.2) *was verified for all resolutions up to* $K = 16$. The explicit test up to $K = 16$ seems sufficient to conclude that DLCQ reproduces in one-to-one fashion the exact solutions of the Schwinger model also in the *continuum limit.*

Diagonalization also gives the *eigenfunctions.* An inspection of the numerical results reveals simple correlations which we can give in closed form. Three examples might suffice. The eigenstate with eigenvalue $M = 1$ has the structure

$$|\Psi_1\rangle = \left|\widetilde{K}\right\rangle = \frac{1}{\sqrt{K}} \sum_{n=0}^{K-1} b_n^\dagger d_{K-n}^\dagger \, |v\rangle \quad . \tag{4.4}$$

No other eigenstate was observed being built up only by two particle Fock states. The next higher states can be interpreted as two-boson configurations. According to Eq. (4.3) one has exactly $K/2$ states of this kind, and the two lowest among them have the eigenstates

$$\begin{aligned} |\Psi_2\rangle = \left|\widetilde{K_2}^2\right\rangle = \frac{\sqrt{2}}{K}\Big\{ &- \sum_{n=0}^{K_2-1} b_n^\dagger d_{K-n}^\dagger + \sum_{n=K_2}^{K-1} b_n^\dagger d_{K-n}^\dagger \\ &+ 2 \sum_{m=0}^{K-1} \sum_{n=1}^{K_2-m-1} b_m^\dagger b_{m+n}^\dagger d_{K_2-m-n}^\dagger d_{K_2-m}^\dagger \Big\} |v\rangle \end{aligned} \tag{4.5}$$

and

$$
\begin{aligned}
|\Psi_3\rangle &= \left|\widetilde{K_2}-\tilde{1},\widetilde{K_2}+\tilde{1}\right\rangle \\
&= \frac{1}{\sqrt{K_2^2-1}}\Big\{-\sum_{n=0}^{K_2-2} b_n^\dagger d_{K-n}^\dagger + \sum_{n=K_2+1}^{K-1} b_n^\dagger d_{K-n}^\dagger \\
&\qquad - \sum_{n=0}^{K_2-2} b_n^\dagger b_{n+1}^\dagger d_{K_2-n-1}^\dagger d_{K_2-n}^\dagger \\
&\qquad + \sum_{m=0}^{K_2-2}\sum_{n=3}^{K_2-m} b_m^\dagger b_{m+n}^\dagger d_{K_2-m-n+1}^\dagger d_{K_2-m-1}^\dagger \\
&\qquad + \sum_{m=0}^{K_2-3}\sum_{n=1}^{K_2-m-2} b_m^\dagger b_{m+n}^\dagger d_{K_2-m-n-1}^\dagger d_{K_2-m+1}^\dagger \Big\}|v\rangle \quad ,
\end{aligned}
\tag{4.6}
$$

with eigenvalues given by Eq. (4.3).

Precisely the same eigenfunctions are obtained if one identifies the bosons of Eq. (4.2) with superpositions of $f\bar{f}$ pairs, *i.e.*

$$
a_n^\dagger = \frac{1}{\sqrt{n}}\left(\sum_{m=0}^{n-1} b_m^\dagger d_{n-m}^\dagger + \sum_{m=0}^{\infty} b_{n+m}^\dagger b_m - \sum_{m=1}^{\infty} d_{n+m}^\dagger d_m\right) \quad , n \geq 1 \ , \tag{4.7}
$$

in terms of which the Hamiltonian, Eq. (2.10) becomes simply

$$
H = m^2 \sum_{n=1}^{\infty} \frac{1}{n}\left(b_n^\dagger b_n + d_n^\dagger d_n\right) + \frac{g^2}{\pi}\sum_{n=1}^{\infty}\frac{1}{n} a_n^\dagger a_n \tag{4.8}
$$

in the charge zero sector. (See also Bergknoff.[24])

It is interesting to note that the first eigenstate with six particle Fock states has a mass $M \geq 3$. Equality holds if the total momentum is shared equally by the three bosons.

One can check that the above pattern of solutions hold for every K; thus, these features hold also in the continuum limit and represent exact solutions. The

fact that the spectrum in DLCQ is obtained correctly even at the very smallest values of K where the wavefunction is only resolved in a gross fashion seems remarkable; in fact this result is special to the Schwinger model and is due to the fact that the wavefunction of the boson is local and thus independent of the fermion momentum. We return to this point in Chapter 6.

5. QUANTUM ELECTRODYNAMICS IN ONE SPACE AND ONE TIME DIMENSION

In this chapter we apply the DLCQ method to the massive Schwinger model: QED_2 with finite mass fermions. It is natural to choose massive fermion states with nonzero k^+ as the Fock state basis. Unless stated otherwise, we will express the mass eigenvalues in units of the Schwinger boson mass $\widetilde{m}$.

5.1 FREE FERMION PAIRS AT WEAK COUPLING.

For $\lambda^2 \ll 1$ the mass operator reduces to the diagonal form $M^2 = KH_0$. The spectrum is illustrated in Fig. 2 for different values of K. The lowest possible mass is obtained if the total momentum $K = 2K_2$ can be shared equally by a fermion and an antifermion, corresponding to the two particles at rest relative to each other. As in the bosonic case, one can construct a band of states for two particles in relative motion, *i.e.*

$$\left(M^2 - \frac{4}{1-(n/K_2)^2}\right)\left|K_2 - n; \bar{K}_2 + \bar{n}\right\rangle = 0\ , \qquad \text{for } n = 0, \ldots, K_2 - 1. \quad (5.1)$$

Contrary to the bosonic case, however, each of the eigenvalues is twofold degenerate for $n \geq 1$ since $\left|K_2 + n; \bar{K}_2 - \bar{n}\right\rangle$ is a different state with the same eigenvalue. As is clear from figure 2, one can also identify bands with three or more particles.

For any specific resolution K, the spectrum is of finite dimension. The highest possible mass state is obtained by putting N fermions and antifermions into the lowest possible momentum states $\left|1,2,\ldots,N;\bar{1},\bar{2},\ldots,\bar{N}\right\rangle$. This state has total momentum $K = N(N+1)$ and an invariant mass

$$M^2 = 2K\sum_{n=1}^{N}\frac{1}{n}. \tag{5.2}$$

The largest mass in the spectrum is thus proportional to $\sqrt{K\log K}$ as opposed to the boson case where it is linear in K. The exclusion principle prohibits a condensate.

The *continuum limit* of the spectrum is fairly obvious from Fig. 2 and from Eq. (5.2). The continuum of masses can be disentangled into multidegenerate continuous bands of states starting at $M = 2,4,\ldots$, corresponding to the relative motion of two or more fermions.

5.2 THE CONTINUUM LIMIT FOR FINITE COUPLING.

In both the weak and the strong coupling limit one can discuss the analytic solution to QED_2 terms of non-interacting particles, fermion pairs in one limit and bosons in the other. In the intermediate region $0 < \lambda < 1$, the solutions can be given numerically.

The lowest mass eigenvalues are displayed as function of λ in the left part of Fig. 3 . They are obtained from numerical diagonalization of the full mass matrix for $K = 16$. The results of a lattice gauge calculation[26] are inserted into the figure as reference points. The comparison with previous numerical work is discussed in greater detail in the next section.

For small λ the spectra can be identified as the continuation of the free solutions (Fig. 2), but they obviously disagree in the strong coupling limit. The higher mass states obviously suffer from poor resolution; i.e.: insufficiently large K. Increasing K presents the difficulty that the matrix dimensions increase exponentially; see for example Table 3. However, as we show below, a simple approximation based on projection onto the lowest number valence Fock component can be used to greatly accelerate the convergence to the continuum limit.

The eigenfunctions of the entire spectrum are obtained as a byproduct of diagonalization in the DLCQ method. As one can see by inspection for resolutions up to $K = 16$, the lowest eigenstates are built mostly from the $|1f;1\bar{f}\rangle$ Fock states. The amplitudes of the four particle states, *i.e.* $|2f;2\bar{f}\rangle$, or of larger particle numbers are very much smaller, typically by 2—3 orders of magnitude. The strength of the two-particle states saturates the unitary bound up to a small fraction. Therefore one can diagonalize the Hamiltonian in the projected $|1f;1\bar{f}\rangle$ space to a high degree of accuracy. The eigenvalues obtained in this manner agree with the full solutions for almost all values of the interaction strength. Only at $\lambda = 1$ and its immediate vicinity is the approximation somewhat less quantitative, since the exact wave functions of the high mass states have significant contributions from the $|2f;2\bar{f}\rangle$ states; see Eqs. (4.5) and (4.6).

The spectrum of the projected space is shown in the right part of Fig. 3 for the comparatively large value of $K = 128$. Despite the large resolution it is rather similar to the left part.

In general the rate of convergence in K depends on the interaction strength. Indeed, if one plots the mass of the lowest state as function of λ for different values of the resolution as done in Fig. 4, the curves coincide almost completely

for $\lambda \lesssim 0.9$. However, for $\lambda \sim 1$, the convergence to the exact value of the lowest mass "vector" state ($M_1 = 1$) is rather slow.

On the other hand one knows from section 4, that the exact value at $\lambda = 1$ is reproduced for *any* value of K provided the quasi-fermion is included. Therefore, we repeated the above calculations using the *massless* fermion representation; the results are plotted in the same figure. Now the vector mass is reproduced exactly for $\lambda = 1$, but for slightly smaller values (say $\lambda \sim 0.9$) the *massless* representation converges even *slower from below* than the *massive* representation converges from *above*. The discrepancy between the two representations is a strong function of λ. For $K = 240$ it decreases from about 40 percent at $\lambda = 1$ to about 10 percent at $\lambda \sim 0.9$ and reduces to a fraction of a percent for $\lambda \sim 0.7$.

The two representations coincide in the limit $K \to \infty$. This can be shown by replacing summation with integration which converts the matrix equation $H_{LC}\Psi = M^2\Psi$ into an integral equation. Restricting to the $(1f; 1\bar{f})$ space one arrives at the same integral equation as Bergknoff,[24] details being given elsewhere.[32] . The lowest mass eigenvalue is displayed in Fig. 4 and represents the *continuum limit.*

The excited states show a similar behavior. In Fig. 5 the lowest members of the *renormalized spectrum* M_i/M_1 are plotted as function of K at two values of λ. Again, one notes a faster convergence in the massive representation than in the massless one, but for sufficiently large K they do yield the *same* value.

One concludes that the continuum limit exists and that the massive representation converges faster for almost all interactions except in the immediate vicinity of the Schwinger point. The continuum limit does not yield new qualitative aspects, such as new states being pulled down from the continuum into the

low mass region.

5.3 COMPARISON WITH EARLIER WORK

The quantitative aspects of the DLCQ approach can be checked by comparison with other work.[17–24]

Tables 4 and 5 collect all the results of Bergknoff[24], recast into the units used here. They agree with the present results to within about one percent, except one point in Table 4 where the discrepancy is about 6 percent. One is tempted to interprete Bergknoff's results for $\lambda = 0.707$ and $\lambda = 0.981$ as printing errors, since they drop out from the systematics of the recalculated values displayed in Fig. 4.

The *renormalized spectrum* as given in Table 5 agrees with the present result within the accuracy quoted by Bergknoff.

Due to the work of Crewther and Hamer[26] a comparison with a lattice gauge calculation is possible. The latter is believed to be the most quantitative among the nonperturbative methods and is in some ways complimentary to the present approach. On the lattice one discretizes in usual space and quantizes at usual time, as opposed to DLCQ where one discretizes in momentum space and quantizes at equal light cone time. It is therefore rather significant the lattice gauge results agree by and large with the present results as displayed in Table 6.

It seems inherent to the numerical part of the lattice calculation that the vector mass m_- (lowest state) can be calculated more precisely than the scalar mass m_+ (second state). Crewther and Hamer quote precisions of 1-2 and 1-5 percent, respectively. The higher mass states have not been calculated so far. The values compiled in Table 6 are taken from a figure, in which the authors

plot what they call the binding energy $E_\pm \equiv (m_\pm - 2m)/g$. The additional uncertainty is estimated to about 1-2 percent. The values of $E_\pm$ in the original units are displayed in the table together with the values of $m_\pm$ in our units, which can be compared with the present results for M_1 and M_2.

Within the limits of error defined above, the lattice gauge calculation agrees with the DLCQ values for both the vector and the scalar state for all interactions except at the largest values of $\lambda = 0.976$. The discrepancy of the vector mass ($\sim 8\%$) can be explained easily by an insufficiently large K. The continuum calculation for the vector mass dispayed in Fig. 4 agrees quite well with the lattice gauge calculation for *all* interactions λ.

6. THE MASS SPECTRUM AND STRUCTURE FUNCTION IN QED_2

As we have shown in the previous section, by restricting the Fock basis to the $|1f;1\bar{f}\rangle$ space, the spectrum is considerably simplified, and the lowest set of mass eigenvalues are still obtained with high accuracy. What is the role of these approximate states as compared to the full solution? Having established the continuum limit and the quantitative aspects of the DLCQ approach, one can treat this question qualitatively for the comparatively small value of $K = 16$.

Fig. 6 shows the 124 masses of the full Fock space for all possible interactions. We interpret the complex spectrum of the full space as follows. The (massive) Fock space for $K = 16$ contains Fock states with at most six particles, *i.e.* 18 $|3f;3\bar{f}\rangle$ states. As we discussed in section 5 one expects for small coupling the onset of a continuum band of states beginning at $M = 3$, which is hidden in the continuum of the band starting at $M = 2$. (See also Fig. 2.) The latter

correspond to the 91 $|2f;2\bar{f}\rangle$ states. It is remarkable that the band at $M \geq 2$ persists for all values of the interaction. Finally, the band of the 15 $|1f;1\bar{f}\rangle$ states starts at $M = 1$.

The particle number seems to be important for the interpretation of the spectrum. This surmise is supported both by inspection of the wavefunction and by the following auxiliary calculation. In the left part of Fig. 7 we have plotted the masses as obtained from diagonalization within only the $(1f;1\bar{f})$ space, and in the right part those obtained from diagonalizing within the $(2f;2\bar{f})$ space alone. It is amazing to see how every state in Fig. 7 finds its analogue in Fig. 6. Ignoring the regime where crossing points occur, there is good quantitative agreement in the respective spectra.

The full spectrum of Fig. 6 can thus be disentangled into two distinct components. The $(1f;1\bar{f})$ component stays discrete even in the continuum limit. (See also the discussion in the preceeding section.) The discrete states can be understood as intrinsic exitations of a meson or positronium-like system. In analogy to the Schwinger model, the second component of the $(2f;2\bar{f})$ states can be interpreted as continuum scattering states with nonzero relative motion of two bosons. The residual interactions, the matrix elements $\langle 1f;1\bar{f}| H |2f;2\bar{f}\rangle$ generate mixtures of these two components, which obviously have not much impact on the mass eigenvalues except at the crossing points.

The Schwinger model has a mass gap between $M = 1$ and $M = 2$. In the massive theory this gap is now occupied by bound states, the mentioned excitations of a positronium-like system. For $M \geq 2$ they are potentially unstable, decaying by a small perturbation into two or more effective bosons. Further analysis in terms of decay rates and branching ratios requires further development

of scattering theory within the DLCQ framework. (See e.g. the recent work at equal time of Kröger.[31])

One of the most important advantages of the DLCQ method is the fact that the wavefunctions required for calculating scattering amplitudes, current matrix elements, form factors, etc. are obtained automatically as the eigenfunction coefficients C_i^j of Eq. (3.4). It is interesting to report one representative example where the eigenfunctions are needed, *i.e.* the bound state structure function appearing in deep inelastic lepton scattering. The structure function $f(x)$ is the probability to find a fermion carrying the fraction x of the total momentum P^+. Since $x = p^+/P^+$, *i.e.* $x = n/K$ one has

$$f_i(x)dx = \langle M_i, K | b_n^\dagger b_n | M_i, K \rangle = \sum_j |C_i^j|^2 \langle \Phi_j | b_n^\dagger b_n | \Phi_j \rangle \quad \text{at } x = \frac{n}{K} \quad , \ (6.1).$$

The normalization is fixed by the requirement $\int_0^1 dx\, f_i(x) = 1$. The matrix element $\langle \Phi_j | b_n^\dagger b_n | \Phi_j \rangle$ is 1 or 0 depending on whether or not the fermion state n is occupied in $|\Phi_j\rangle$.

The structure function for the lowest state $f(x) \equiv f_1(x)$ is plotted in Fig.8 for various values of λ. The results show the transition from weak coupling, nonrelativistic dynamics at small λ to the broad distribution expected for highly relativistic binding at large λ. As a consequence of discretization, the support is discrete, and f is a distribution rather than a function; in practice this is irrelevant for large resolution. The results shown here are for $K = 240$.

In QED_2 the lowest eigenstate is dominated by the two-fermion Fock component; *i.e.*, two "quarks". The structure function is thus peaked close to $x = \frac{1}{2}$ and it is approximately symmetric in x about this point. At $x = 1$ the structure function is strictly zero since the highest possible momentum state for the

fermion is $K-1$, *i.e.* $b^\dagger_{K-1}d^\dagger_1|v\rangle$. We find that the contribution of higher Fock states to the lowest mass state structure function is strikingly small. The ratio of probabilities of all the higher particle number states relative to the valence Fock state never exceeds 10^{-4} at any λ and $K \leq 16$. This can be understood from the fact that at both very low and very high couplings the bound state consists of only two fermions.

At $\lambda = 1$, QED_2 becomes the Schwinger model. As indicated in section 4, in this case the structure function is a constant: $f(x) = 1$; *i.e.* the quasifermion has the same occupation number in all other momentum states. The bound state is thus local in position space. We note that our results are in fair agreement with the structure function displayed by Bergknoff.[24]

The details of the higher Fock space contributions to the structure function as well as other properties of the eigenstates such as distribution amplitudes or charge distribution functions will be given separately.[32]

7. SUMMARY AND CONCLUSIONS

The basis of the Discretized Light Cone Quantization Method (DLCQ)[1] for solving field theories is conceptually simple: One quantizes the independent fields at equal light cone time τ and requires them to be periodic in light cone space with period $2L$. The commuting operators, the light cone momentum $P^+ = \frac{2\pi}{L}K$ and the light cone energy $P^- = \frac{L}{2\pi}H$ are constructed explicitly in a Fock space representation and diagonalized simultaneously. The eigenvalues give the physical spectrum: the invariant mass squared $M^2 = P^\nu P_\nu$. The eigenfunctions give the wavefunctions at equal τ and allow one to compute the current matrix elements, structure functions, and distribution amplitudes required for physical

processes. All of these quantities are manifestly independent of L, since $M^2 = P^+P^- = HK$. Lorentz-invariance is violated by periodicity, but reestablished at the end of the calculation by going to the continuum limit: $L \to \infty$, $K \to \infty$ with P^+ finite. In the case of gauge theory, the use of the light cone gauge $A^+ = 0$ eliminates negative metric states in both abelian and non-abelian theories.

As we have shown in this paper the application of DLCQ to a gauge invariant Abelian field theory like QED_2 is straightforward. For any given resolution K the number of contributing Fock states is finite because of the positivity of the light cone momenta and the Pauli principle (in the case of massless fermions). No unexpected problems appear in the calculations. QED_2 in $A^+ = 0$ gauge is much simpler than the scalar Yukawa field theory,[2] since the transverse degrees of freedom and therefore the photons are absent in 1+1 dimensions. One can see immediately in the DLCQ approach that QED_2 has an arbitrary mass scale. This scale can be adjusted by (re)normalizing the lowest mass to an arbitrary but fixed value.

We have also established precise agreement between the DLCQ results and the exact solutions of the Schwinger model proper at any resolution K, as well as in the continuum limit. This result gives further evidence that quantizing a system at equal light cone time is equivalent to quantizing it at equal usual time.

In the case of the massive Schwinger model (QED_2), we established the existence of the continuum limit numerically; for sufficiently large resolution K the results become independent of K. The essential criteria for convergence is that the intrinsic dynamical structure of the wavefunctions is sufficiently resolved at the rational values $x = n/K, n = 1, 2, ..K-1$ accessible at a given K. Unlike the case in the usual space-time methods, the size of the discretization or lattice

length scale L, is irrelevant.

In the large K limit, the eigenvalues agree quantitatively with the results of Bergknoff[24] and with those of a lattice gauge calculation by Crewther and Hamer.[26] This result is important in establishing the equivalence of different complementary nonperturbative methods.

We also verified numerically that different Fock space representations yield the same physical results. In particular we solved the QED_2 spectrum in the space corresponding to the solutions of the free, massive Dirac equation $(i\gamma^\mu\partial_\mu + m_F)\psi = 0$ as well as of the massless equation $i\gamma^\mu\partial_\mu\psi = 0$. We only found convergence problems for the very large coupling regime λ near 1 .

Even for moderately large values of the resolution, DLCQ provides one with a qualitatively correct picture of the whole spectrum of eigenfunctions. This aspect becomes important for the development of scattering theory within the DLCQ approach. For example we have found the rather surprising result that the lowest eigenfunction has virtually no components of $|2f;2\bar{f}\rangle$ and higher particle Fock states (*i.e.* no 'sea quarks'). The structure functions for the sea quarks will be given in a separate paper.

There are a number of important advantages of the DLCQ method which have emerged from this study of two-dimensional field theories.

(1) The Fock space is denumerable and finite in particle number for any fixed resolution K. In the case of gauge theory in 3+1 dimensions, we expect that photon or gluon quanta with zero 4-momentum decouple from neutral or color-singlet bound states, and thus need not be included in the Fock basis. The transverse momenta are additive and can be introduced on a cartesian grid. We are currently developing methods to implement the color degrees of freedom for

the non-Abelian theories.

(2) Unlike lattice gauge theory, there are no special difficulties with fermions: e.g., no fermion doubling, fermion determinants, or necessity for a quenched approximation. Furthermore, the discretized theory has basically the same ultraviolet structure as the continuum theory. We emphasize that unlike lattice calculations, there is no constraint or relationship between the physical size of the bound state and the length scale L.

(3) The DLCQ method has the remarkable feature of generating the complete spectrum of the theory; bound states and continuum states alike. These can be separated by tracing their minimum Fock state content down to small coupling constant since the continuum states have higher particle number content. In lattice gauge theory it appears intractable to obtain information on excited or scattering states or their correlations. The wavefunctions generated at equal light cone time have the immediate form required for relativistic scattering problems.

(4) DLCQ is basically relativistic many body theory, including particle number creation and destruction, and is thus a basis for relativistic nuclear and atomic problems. In the non-relativistic limit the theory is equivalent to many-body Schrödinger theory.

The immediate goal is gauge theory in 3+1 dimensions. Even in the Abelian case it will be interesting to analyze QED and the positronium spectrum in the large α limit. Whether the non-Abelian theory can be solved using DLCQ – considering its greater number of degrees of freedom and its complex vacuum and symmetry properties is an open question. The studies we have reported here for Abelian gauge theory in 1+1 dimensions do give some grounds for optimism.

ACKNOWLEDGEMENTS

This research was supported in part by the Department of Energy, contract DE-AC03-76SF00515, by the National Science Foundation under Grant No. PHY82-17853 and supplemented by funds from the National Aeronautics and Space Administration. Two of the authors (H.C.P. and S.J.B.) have enjoyed helpful discussions with K. Hornbostel, V. Nair, F. Lenz, S. Koonin and U. Heller at the QCD Program of the Institute for Theoretical Physics, at the University of California in Santa Barbara. They thank the staff of the ITP for providing such a stimulating atmosphere.

APPENDIX The Matrix Elements $\{m|n\}$ and $[m|n]$.

The inverse derivative $(i\partial_\xi)^{-1}$ is introduced for notational convenience but stands for a Green's function or a propagator in the following sense. Suppose a function $g(\xi,\eta)$ is given for all values of ξ and η. The unknown function $\phi(\xi,\eta)$ is to be determined by $i\partial_\xi\phi = g$ or by $\phi = \frac{1}{i\partial_\xi}\, g$. This can be achieved by means of a Green's function $G(\xi,x) = \frac{i}{2}\,\epsilon(\xi - x)$ which solves $i\partial_\xi G(\xi,x) = \delta(\xi - x)$, *i.e.*

$$\phi(\xi,\eta) = \int_{-\infty}^{+\infty} dx\; G(\xi,x)\; g(x,\eta) + C \quad , \tag{A1}$$

the arbitrary constant C being a solution to the homogeneous equation.

The inverse derivative has a property of a partial derivative. Consider $I \equiv \int d\xi(\partial_\xi^{-1} f)\partial_\xi V$. Integrate partially to get $I = (\partial_\xi^{-1} f)\, V \; - \int d\xi\, f\, V$. Substitute

$V \equiv \partial_\xi^{-1} g$ and get

$$\int d\xi \, (\partial_\xi^{-1} f)\, g = (\partial_\xi^{-1} f)(\partial_\xi^{-1} g) - \int d\xi \, f \, \partial_\xi^{-1} g \quad , \tag{A2}$$

i.e. the inverse partial can be shifted from f to g without changing their order.

These properties can be used to evaluate the matrix element $\{m|n\}$ as defined by $\{m|n\} \equiv \frac{1}{2\pi} \int_{-\pi}^{+\pi} d\xi \; e^{im\xi} \; \frac{1}{i\partial_\xi} \; e^{in\xi}$. In choosing boundary conditions such that the constant C in Eq. (A1) vanishes, one arrives straightforwardly at

$$\{m|n\} \begin{cases} = \frac{1}{m} \, \delta_{m+n,0} & \text{if } m \neq 0 \text{ and } n \neq 0 \\ = 0 & \text{if } m = 0 \text{ or } n = 0 \end{cases} \quad . \tag{A3}$$

We use the opportunity to correct an error in ref.2 . There, the limits of integration of the Green's function have been put consistently $(\pm\pi)$ instead of the correct values $(\pm\infty)$ as in Eq. (A1). This error does not affect the final results, since Eq. (A3) was used consistently.

One proceeds similarly with $(i\partial_\xi)^{-2}$, defining $\phi(\xi) \equiv \frac{1}{\partial_\xi^2} \; e^{in\xi}$. The Green's function of the problem is given by $G(\xi, x) = \frac{1}{2} \; |\xi - x|$ and the most general solution by $\phi(\xi) = \frac{1}{2} \int_{-\infty}^{+\infty} dx \; |\xi - x| \; e^{inx} + F\xi + C$, with F and C being arbitrary constants. Boundaries are chosen such that C and F vanish. The integral is not well defined except upon introducing a convergence factor, *i.e.* $\phi(\xi) = \lim_{\kappa \to 0} \; e^{in\xi} \int_0^\infty dx \; e^{-\kappa x} \; \cos nx$ which gives $\phi_\kappa(\xi) = \frac{\kappa^2 - n^2}{(\kappa^2 + n^2)^2} \; e^{in\xi}$. One keeps κ finite, taking the limit at the end.

Having defined $[m|n] \equiv \frac{1}{2\pi} \int_{-\pi}^{+\pi} d\xi \; e^{im\xi} \left(\frac{1}{i\partial_\xi} \right)^2 e^{in\xi}$, one obtains for both $m \neq 0$ and $n \neq 0$

$$[m|n] = \frac{1}{n^2} \, \delta_{m+n,0} \quad , [m|0] = 0 \quad , [0|n] = 0 \quad , [0|0] = -\frac{1}{\kappa^2} \quad . \tag{A4}$$

One notes that $[0|0]$ diverges in the limit $\kappa \to 0$.

In choosing the integration constants F and C one has not much freedom. For self-bound systems one has to omit external fields (*i.e.* $F = 0$); however, see also the work of Coleman.[18,19] For nonzero values of C, the light cone momentum and the energy would *not* commute, as can be verified by explicit calculation.

REFERENCES

1. H. C. Pauli and S. J. Brodsky, Phys. Rev. **D32** (1985) 1993
2. H. C. Pauli and S. J. Brodsky, Phys. Rev. **D32** (1985) 2001.
3. J. B. Kogut and D. E. Soper, Phys. Rev. **D1** (1970) 2901.
4. J. D. Bjørken, J. B. Kogut and D. E. Soper, Phys. Rev. **D3** (1971) 1382.
5. S. J. Brodsky, R. Roskies and R. Suaya, Phys. Rev. **D8** (1973) 4574.
6. S. J. Chang, R. G. Root, and T. M. Yan, Phys. Rev. **D7** (1973) 1133;
   T. M. Yan, Phys. Rev. **D7** (1973) 1760.
7. G. P. Lepage and S. J. Brodsky, Phys. Rev. **D22** (1980) 2157.
8. G. P. Lepage, S. J. Brodsky, T. Huang, and P. Mackenzie
   in Banff 1981, Particle and Fields **2**.
   S. J. Brodsky, in Short-Distance Phenomena in Nuclear Physics (Plenum Publishing Corporation, 1983), p. 141-217.
9. A. Casher, Phys.Rev. **D14** (1976) 452.
10. V.A. Franke, Y.V. Novozhilov, E.V. Prokhvatilov,
    Lett. Math. Phys. **5** (1981) 239,437.
11. Q. Ho-Kim, L. Marleau, and P. Mathieu,
    Print-86-1020 (LAVAL) and Print-86-0312 (LAVAL), 1986.
    Contributed to the 23rd International Conference on High-Energy Physics held in Berkeley, CA, 16-23 July 1986.
12. J. Schwinger, Phys. Rev. **128** (1962) 2425; J. Schwinger, in Theoretical Physics, Trieste Lectures, 1962 (IAEA, Vienna, 1963), p. 89.
13. J. H. Lowenstein and J. A. Swieca, Ann. Phys. (N.Y.) **68** (1971) 172.

14. A. Casher, J. Kogut and L. Susskind, Phys. Rev. **D10** (1974) 732.

15. J. Kogut and L. Susskind, Phys. Rev. **D10** (1974) 3468.

16. N.S. Manton, Ann. Phys. (N.Y.) **159** (1985) 220.

17. J. Kogut and L. Susskind, Phys. Rev. **D11** (1975) 395.

18. S. Coleman, R. Jackie, and L. Susskind, Ann. Phys. (N.Y.) **93** (1975) 267.

19. S. Coleman, Ann. Phys. (N.Y.) **101** (1976) 239.

20. Y. Frishman, in Particles, Quantum Fields and Statistical Mechanics, Proceedings Mexico City 1973, M. Alexanian and A. Zereda, Eds., (Springer-Verlag, Berlin, Heidelberg, New York, 1975), p. 118.

21. K. D. Rothe and J. A. Swieca, Phys. Rev. **D15** (1979) 541;
K. D. Rothe and J. A. Swieca, Ann. Phys. (N.Y.) **117** (1979) 382;
K. D. Rothe and J. A. Swieca, Phys. Rev. **D15** (1979) 1675;
H. J. Rothe, K. D. Rothe and J. A. Swieca, Phys. Rev. **D19** (1979) 3020.

22. I. Bender, H.J. Rothe, and K.D. Rothe, Nucl. Phys. **B251** (1985) 745.

23. A. Schiller and J. Ranft, Nucl. Phys. **B225** (1983) 204.

24. H. Bergknoff, Nucl. Phys. **B122** (1977) 215 .

25. C.J. Hamer, J. Kogut, D.P. Crewther and M.M. Mazzolini,
Nucl. Phys. **B208** (1982) 413 .

26. D.P. Crewther and C.J. Hamer,Nucl. Phys. **B170** (1980) 353 .

27. A.T.M. Aerts and T.H. Hansson, Z.Phys. **C28** (1985) 537.

28. Y. Nakawaki, Progr. Theor.Phys. **70** (1983) 1105.

29. Y. K. Ha, Phys. Rev. **D29** (1984) 1744.

30. G.D. Date, Y. Frishman, and J. Sonnenschein , WIS-86/22-Ph, 1986.

31. H. Kröger, A. Smailagic, and R. Girard, Phys. Rev. **D32** (1985) 3221

32. to be published; and

Th. Eller, PhD thesis, Heidelberg University, to be published.

TABLE CAPTIONS

1. *The invariant mass squared in Fock space representation.* — Both, the diagonal inertia matrix KH_0 and the interaction matrix KV are dimensionless and related to the invariant mass squared by $M^2 = m^2 KH_0 + g^2/\pi KV$. Entries are the Fock states $|i\rangle = |nf; n\bar{f}\rangle$.

2. *Matrix dimensions for different resolutions K.*— The right part of the table gives the contribution to N_{dim} according to the number of fermions in the *massless* representation.

3. *The Schwinger model in boson representation.*— The eigenvalues of the invariant mass squared M_i^2 are given for low resolution K, together with the Fock states for massive bosons.

4. *Comparison with the vector mass of Bergknoff.*[24] — The vector mass (M_V) as calculated by Bergknoff for different $m\sqrt{\pi}/g$ is converted into the present units and compared with DLCQ (M_1) for $K = 240$.

5. *Comparison with the spectrum of Bergknoff.*[24] The first 4 normalized masses $(M_i/M_1)_B$ are compared with the DLCQ results M_i/M_1. Calculations are done at $m\sqrt{\pi}/g = 2$ ($\lambda = 0.447$) for $K = 240$.

6. *Comparison with the results of Crewther and Hamer.*[26] — The so called binding energies $E_\pm$ are interpolated graphically from their Fig. 10, converted to masses $m_\pm \equiv gE_\pm + 2m$ in the present units and compared to the DLCQ results $M_{1,2}$ for $K = 240$.

Table 1: *The invariant mass squared in Fock space representation.*

	KH_0	KV				
		$\|1\rangle$	$\|2\rangle$	$\|3\rangle$	$\|4\rangle$	$\|5\rangle$
$\langle 1\| = \langle 0;\bar{1}\|$	1	1	$K=1$			
$\langle 1\| = \langle 0;\bar{2}\|$	1	$\frac{5}{2}$	$K=2$			
$\langle 2\| = \langle 1;\bar{1}\|$	4	$-\frac{3}{2}$	$\frac{5}{2}$			
$\langle 1\| = \langle 0;\bar{3}\|$	1	$\frac{49}{12}$		$K=3$		
$\langle 2\| = \langle 1;\bar{2}\|$	$\frac{9}{2}$	$-\frac{8}{3}$	$\frac{19}{3}$			
$\langle 3\| = \langle 2;\bar{1}\|$	$\frac{9}{2}$	$-\frac{5}{12}$	$-\frac{8}{3}$	$\frac{49}{12}$		
$\langle 1\| = \langle 0;\bar{4}\|$	1	$\frac{205}{36}$				$K=4$
$\langle 2\| = \langle 1;\bar{3}\|$	$\frac{16}{3}$	$-\frac{15}{4}$	$\frac{37}{4}$			
$\langle 3\| = \langle 2;\bar{2}\|$	4	$-\frac{3}{4}$	$-\frac{15}{4}$	$\frac{37}{4}$		
$\langle 4\| = \langle 3;\bar{1}\|$	$\frac{16}{3}$	$-\frac{7}{36}$	$-\frac{3}{4}$	$-\frac{15}{4}$	$\frac{205}{36}$	
$\langle 5\| = \langle 0,1;\bar{1},\bar{2}\|$	10	$-\frac{5}{9}$	3	-3	$\frac{5}{9}$	$\frac{58}{9}$

Table 2: *Matrix dimensions for different resolutions K.*

		Contribution to N_{dim} from					
K	N_{dim}	$(1f;1\bar{f})$	$(2f;2\bar{f})$	$(3f;3\bar{f})$	$(4f;4\bar{f})$	$(5f;5\bar{f})$	$(6f;6\bar{f})$
1	1	1					
4	5	4	1				
9	30	9	20	1			
16	231	16	140	74	1		
25	1958	25	572	1136	224	1	
36	17977	36	1785	8866	6685	604	1

Table 3: *The Schwinger model in boson representation.*

K	i	M_i^2	$\|\widetilde{n}^m\rangle_i$
1	1	1	$\|\widetilde{1}\rangle$
2	1	1	$\|\widetilde{2}\rangle$
	2	4	$\|\widetilde{1}^2\rangle$
3	1	1	$\|\widetilde{3}\rangle$
	2	9/2	$\|\widetilde{2},\widetilde{1}\rangle$
	3	9	$\|\widetilde{1}^3\rangle$
4	1	1	$\|\widetilde{4}\rangle$
	2	4	$\|\widetilde{2}^2\rangle$
	3	16/3	$\|\widetilde{3},\widetilde{1}\rangle$
	4	10	$\|\widetilde{2},\widetilde{1}^2\rangle$
	5	16	$\|\widetilde{1}^4\rangle$

Table 4: Comparison with the vector mass of Bergknoff.[24]

λ	$\frac{m}{g}\sqrt{\pi}$	$\frac{M_V}{g}\sqrt{\pi}$	M_V	M_1
0.196	5.0	10.50	2.06	2.088
0.447	2.0	4.79	2.14	2.135
0.707	1.0	2.70	1.91	2.018
0.981	0.2	1.50	1.47	1.457

Table 5: Comparison with the spectrum of Bergknoff.[24]

$\frac{M_i}{g}\sqrt{\pi}$	$(\frac{M_i}{M_1})_B$	$\frac{M_i}{M_1}$
4.79	1.00	1.000
5.97	1.25	1.248
6.90	1.44	1.437
7.70	1.61	1.597

Table 6: Comparison with the results of Crewther and Hamer.[26]

$\frac{m}{g}$	λ	E_-	E_+	m_-	M_1	$\frac{m_+}{m_-}$	$\frac{M_2}{M_1}$
2^5	0.018	0.19	0.49	2.006	2.006	1.004	1.004
2^4	0.035	0.25	0.62	2.014	2.013	1.011	1.010
2^3	0.070	0.30	0.77	2.032	2.030	1.038	1.025
2^2	0.140	0.35	0.93	2.067	2.064	1.070	1.060
2^1	0.271	0.41	1.10	2.122	2.114	1.156	1.135
2^0	0.491	0.46	1.19	2.143	2.129	1.296	1.279
2^{-1}	0.748	0.50	1.15	1.990	1.975	1.433	1.497
2^{-2}	0.914	0.52	1.12	1.653	1.675	1.588	1.753
2^{-3}	0.976	0.54	1.11	1.367	1.476	1.721	1.943

FIGURE CAPTIONS

1. *The spectrum of invariant mass for free massive bosons.* — The mass eigenvalues for free bosons are plotted in units of the free boson mass $\widetilde{m} = \frac{g}{\sqrt{\pi}}$ for each fixed value of the resolution K.

2. *The spectrum of invariant mass for free massive fermions.* — The mass eigenvalues for free massive fermions in the charge $Q = 0$ sector are plotted in units of the fermion mass m for each fixed value of the resolution K.

3. *The lowest eight mass eigenvalues versus the interaction* λ. — The mass eigenvalues in units of $\widetilde{m}$, calculated in the massive representation in steps of $\Delta\lambda = 0.05$, are plotted in the *left part* for $K = 16$ ($N_{dim} = 124$) using the full Fock space (see also Fig. 6) and in the *right part* for $K = 128$ ($N_{dim} = 127$) using *only* the $(1f; 1\bar{f})$ part of the Fock space. — The results of the lattice gauge calculation (see table 6) are inserted as reference points. — The dashed curves in the left part represent mass eigenvalues for $K = 16$ with the $(1f; 1\bar{f})$ Fock space.

4. *The continuum limit for the vector mass.* — The vector mass in units of $\widetilde{m}$ is calculated as function of λ with the $(1f; 1\bar{f})$ Fock space in the massless (*lower band*) and the massive representation (*upper band*) for six values of $K = 40, 80, \ldots, 240$. Calculations are done in steps of $\Delta\lambda = 0.01$. — The recalculated continuum limit (similar to ref. 24) is given by the diamonds; the triangles and squares refer to the results of Bergknoff[24] (Table 4) and of the lattice gauge calculation[26] (Table 6), respectively.

5. *The continuum limit for the excited states.* — The normalized masses M_i/M_1 for $i = 2, 3, 4$ as calculated with the projected $(1f; 1\bar{f})$ Fock space in

the massless (*lower curves*) and the massive representation (*upper curves*) are plotted versus the resolution K at two coupling constants $\lambda = 0.491$ (*left*) and $\lambda = 0.748$ (*right*).

6. *The renormalized spectrum of invariant masses.* — The invariant masses M_i/M_1 as calculated with the full Fock space of the massive representation for $K = 16$ is plotted versus *all values* of the coupling constant λ. — Note the qualitatively different parts of the spectrum. Many quasi-crossings are not resolved graphically despite the small step in the calculation, $\Delta\lambda = 0.01$.

7. *Discrete and Continuous spectra.* — The *left part* displays the renormalized masses for $K = 16$ as calculated from the eigenvalues in *only* the $(1f; 1\bar{f})$ Fock space and the *right part* as calculated in *only* $(2f; 2\bar{f})$ Fock space. Both spectra are renormalized with the same $\widetilde{m}(\lambda)$.

8. *The structure function for the lowest eigenstate.* — The structure function is calculated in the massless representation for $K = 128$ and plotted versus the Bjørken variable $x = \frac{p^+}{P^+}$ for different interactions λ.

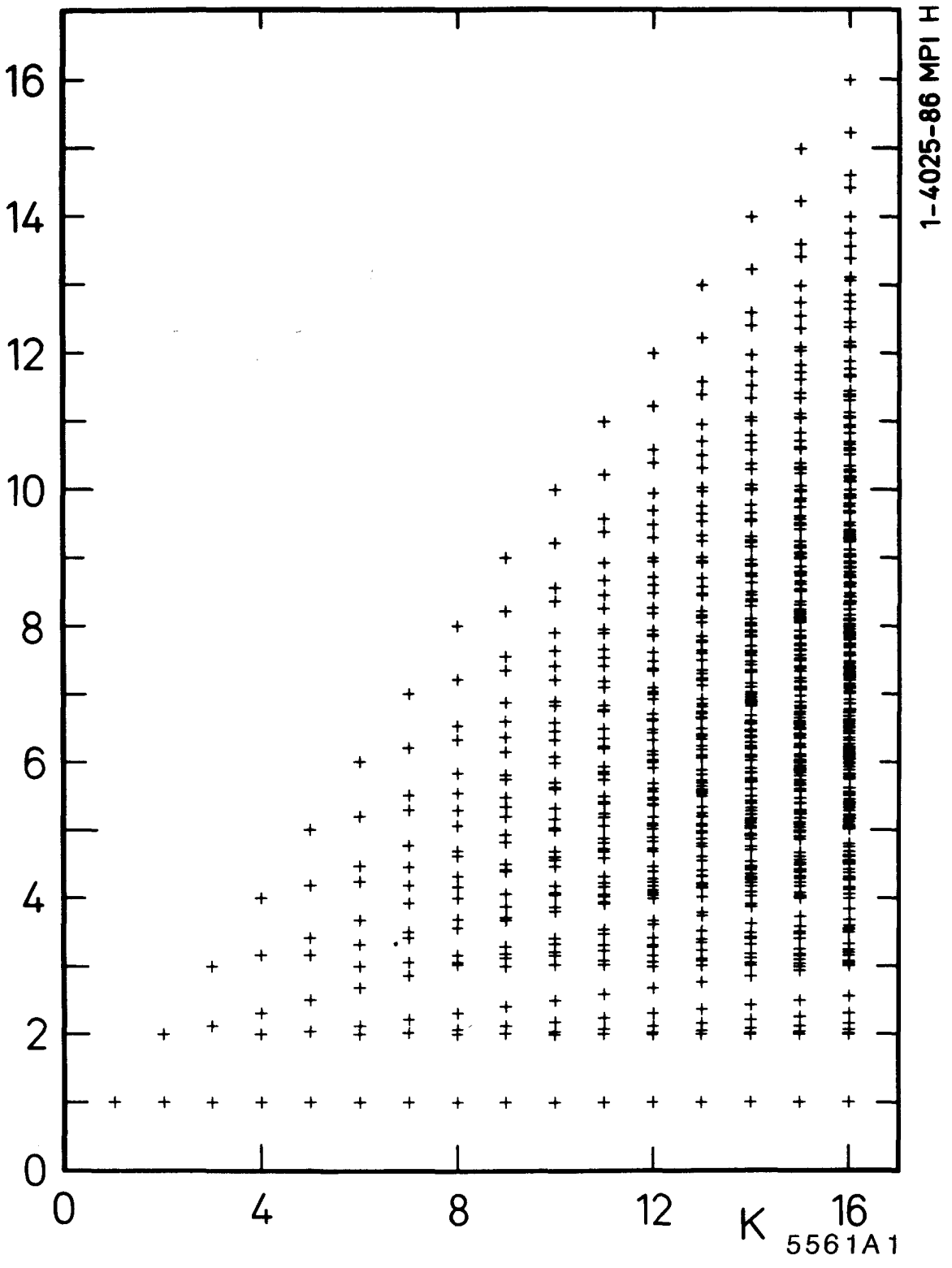

Fig. 1

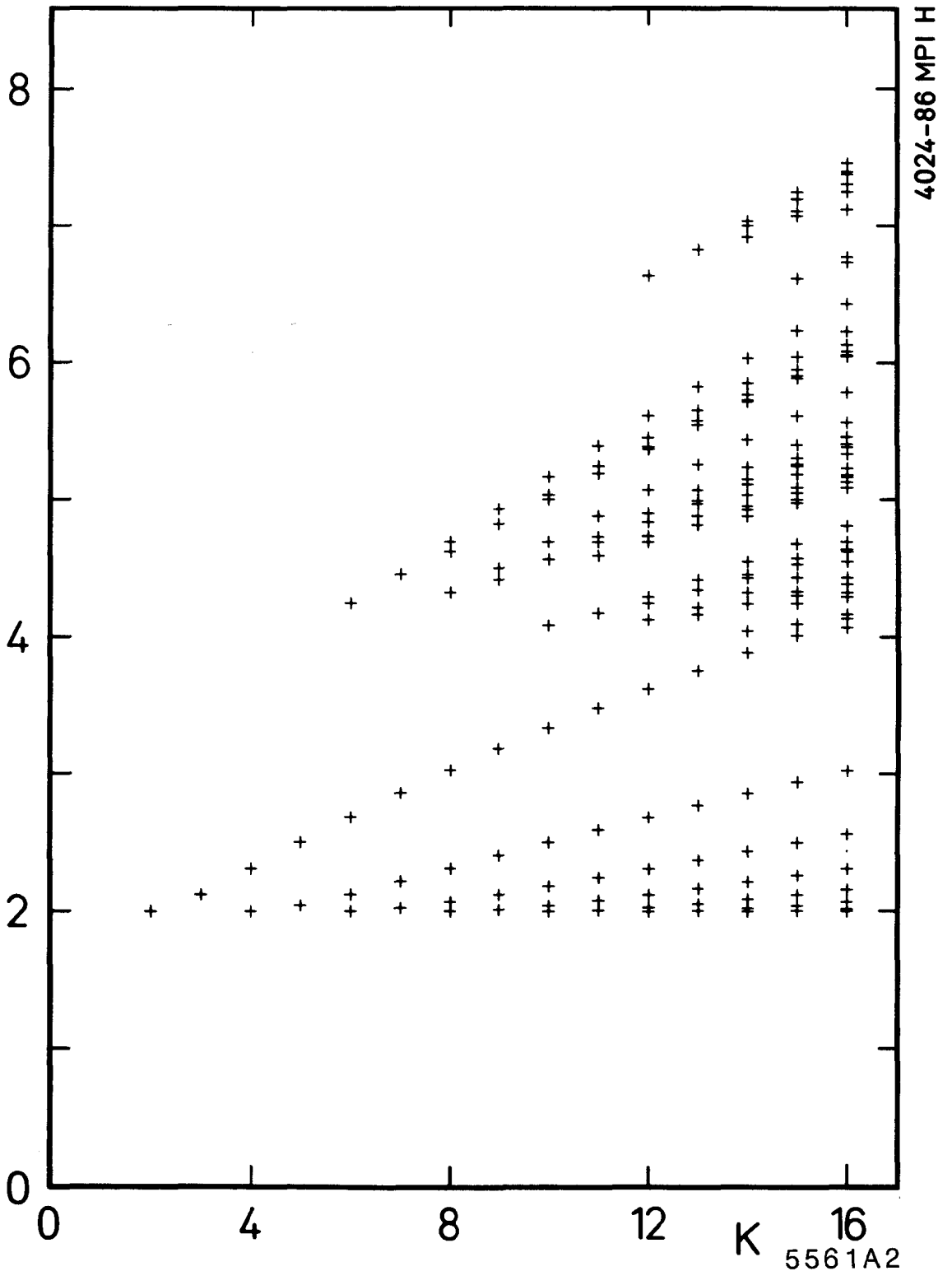

Fig. 2

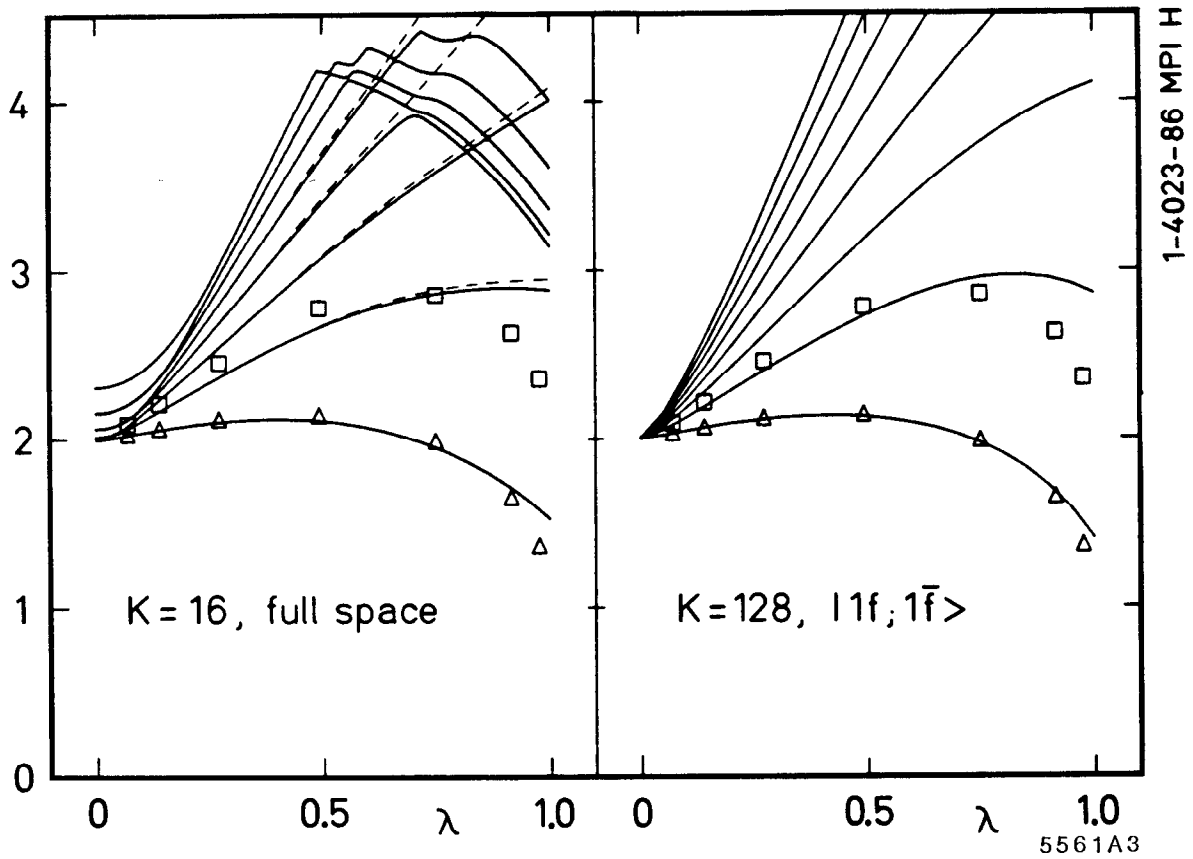
4
3
2
1
0
K = 16, full space
K = 128, |1f; 1f̄>
0
0.5
λ
1.0
0
0.5
λ
1.0
1-4023-86 MPI H
5561A3

Fig. 3

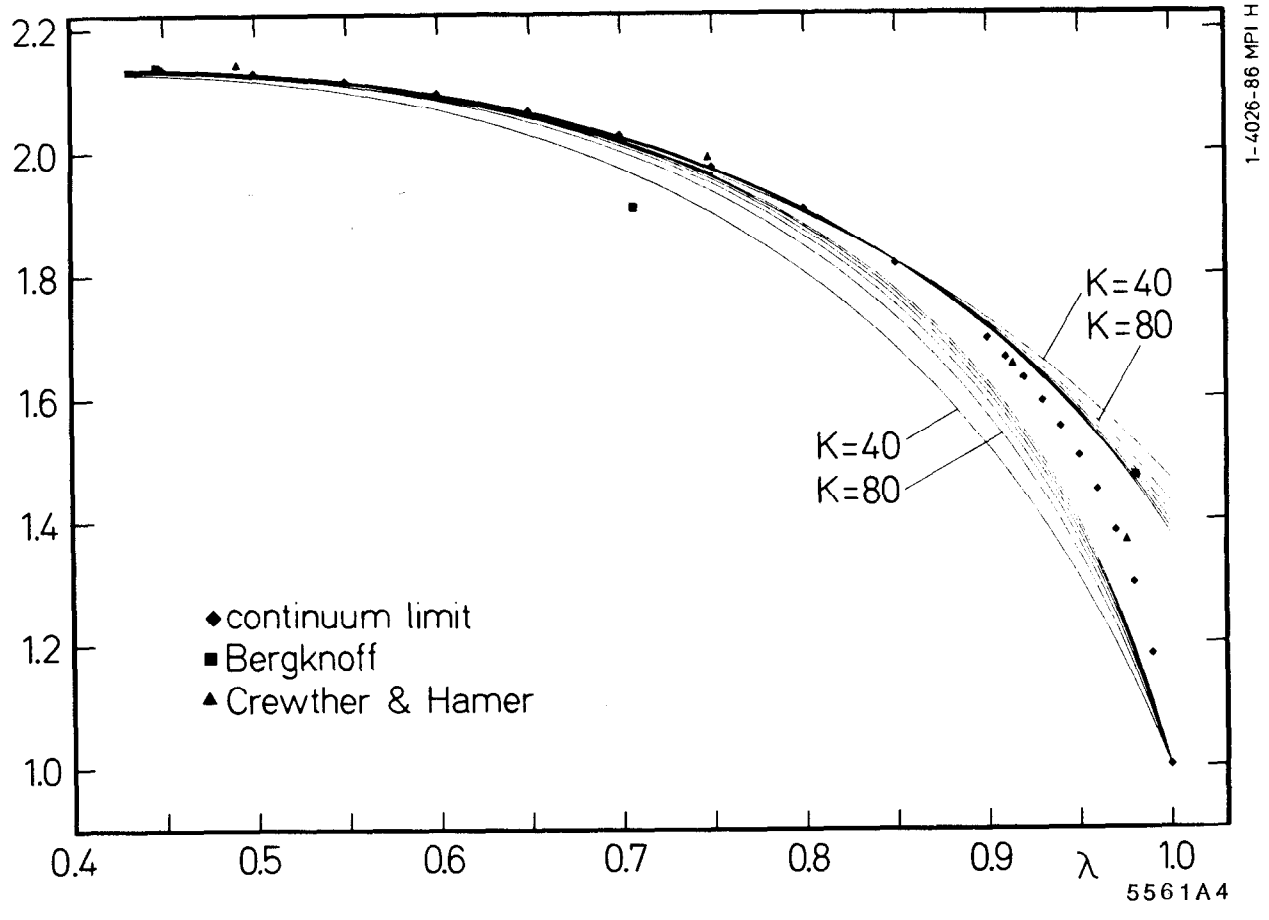
2.2
2.0
1.8
1.6
1.4
1.2
1.0
0.4
0.5
0.6
0.7
0.8
0.9
λ
1.0
K=40
K=80
K=40
K=80
◆continuum limit
■Bergknoff
▲Crewther & Hamer
1-4026-86 MPI H
5561A4

Fig. 4

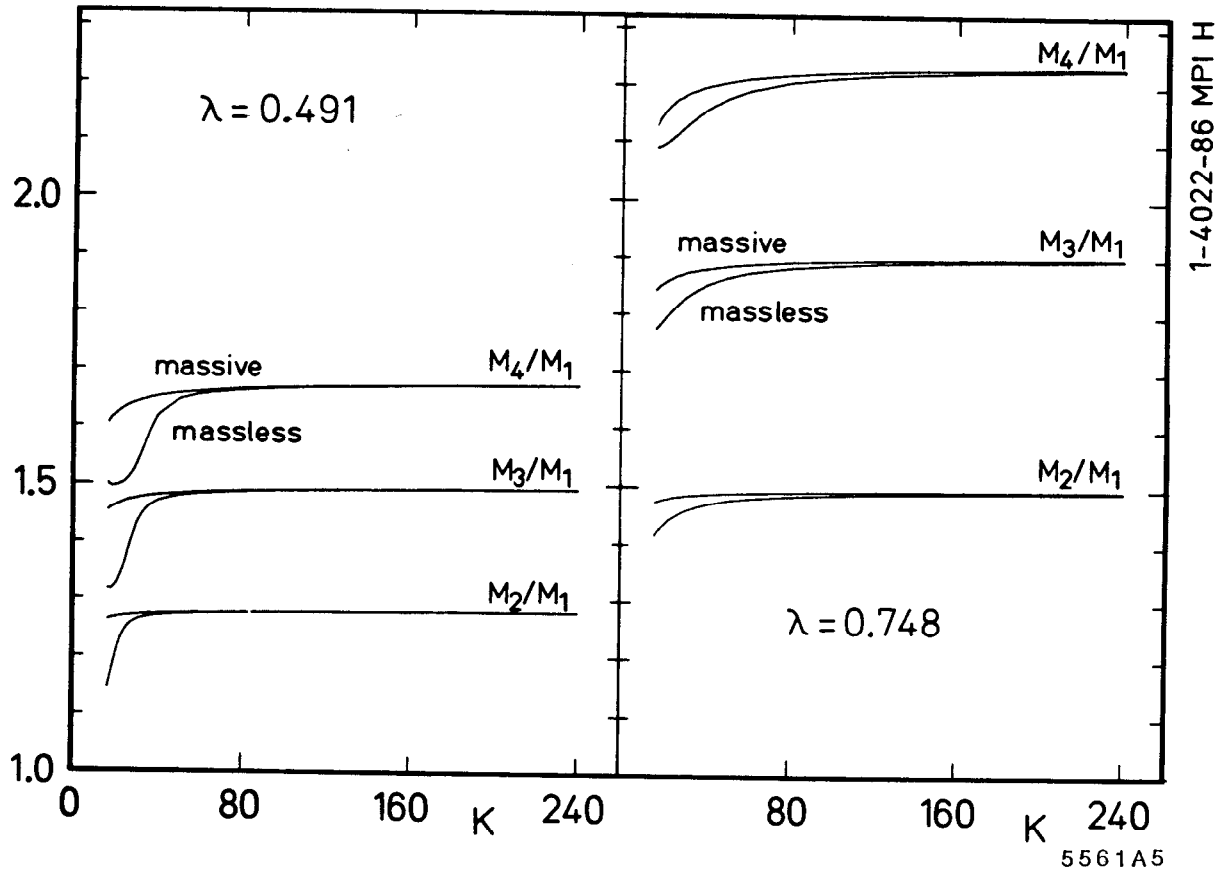
λ = 0.491
λ = 0.748
massive
massless
M_4/M_1
M_3/M_1
M_2/M_1
2.0
1.5
1.0
0
80
160
K
240
1-4022-86 MPI H
5561A5

Fig. 5

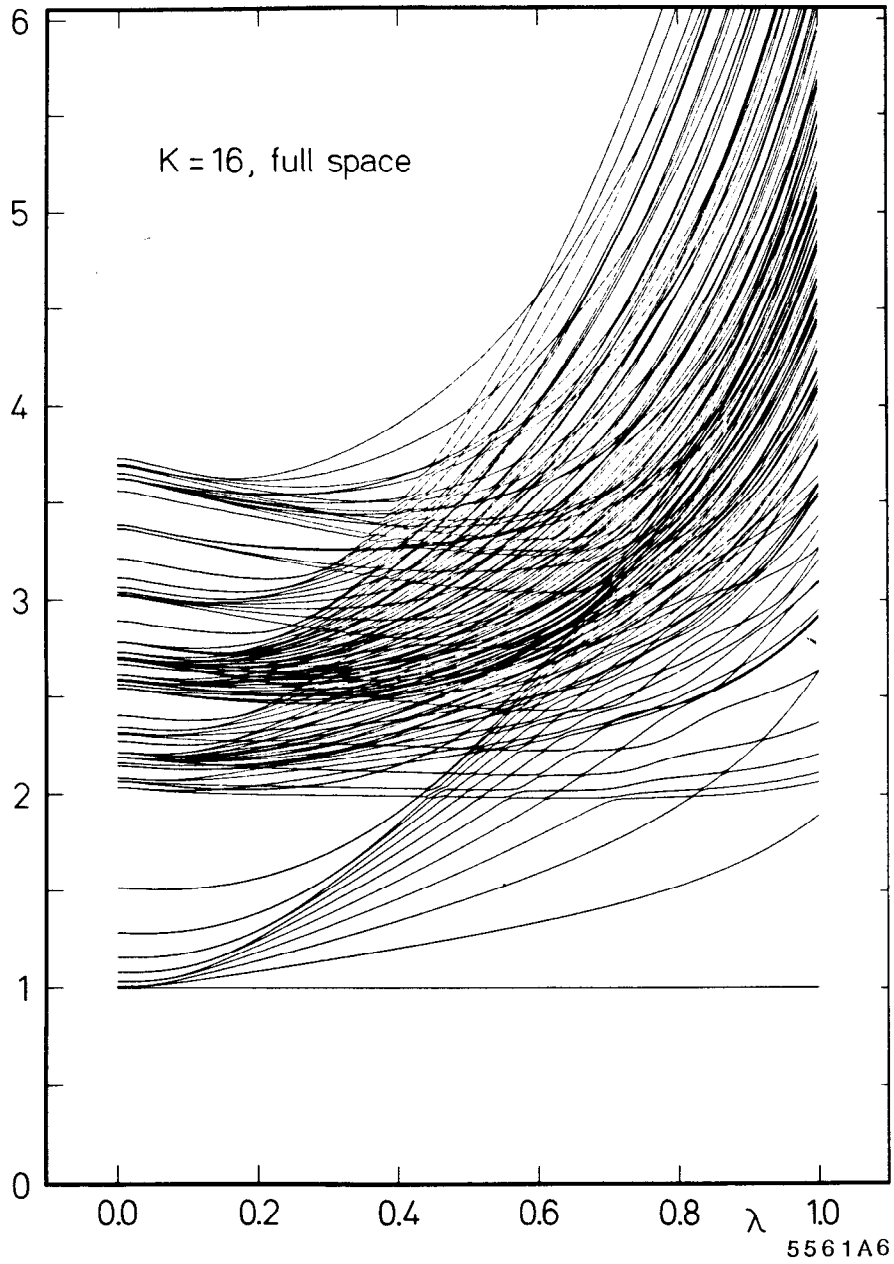

Fig. 6

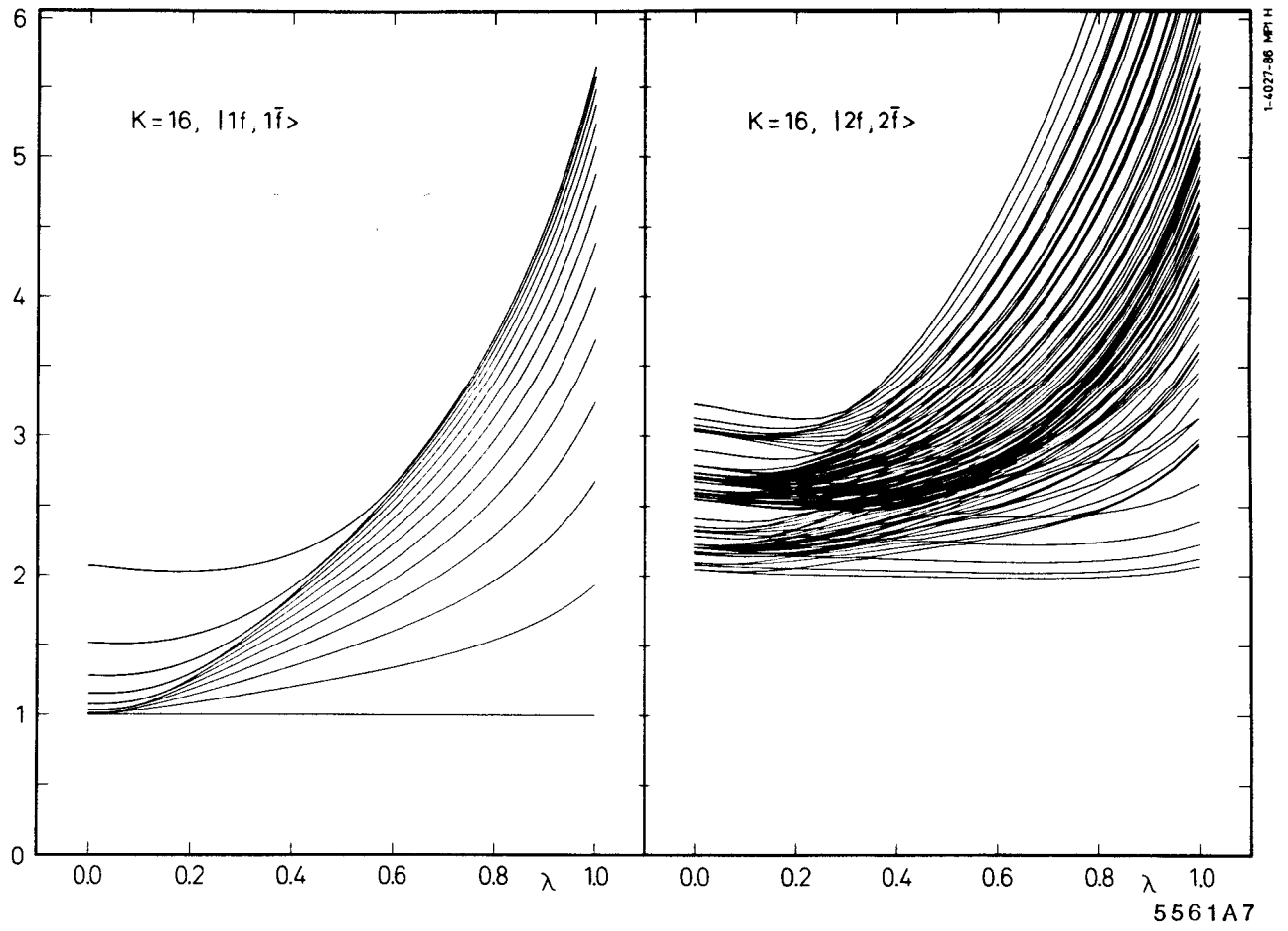

Fig. 7

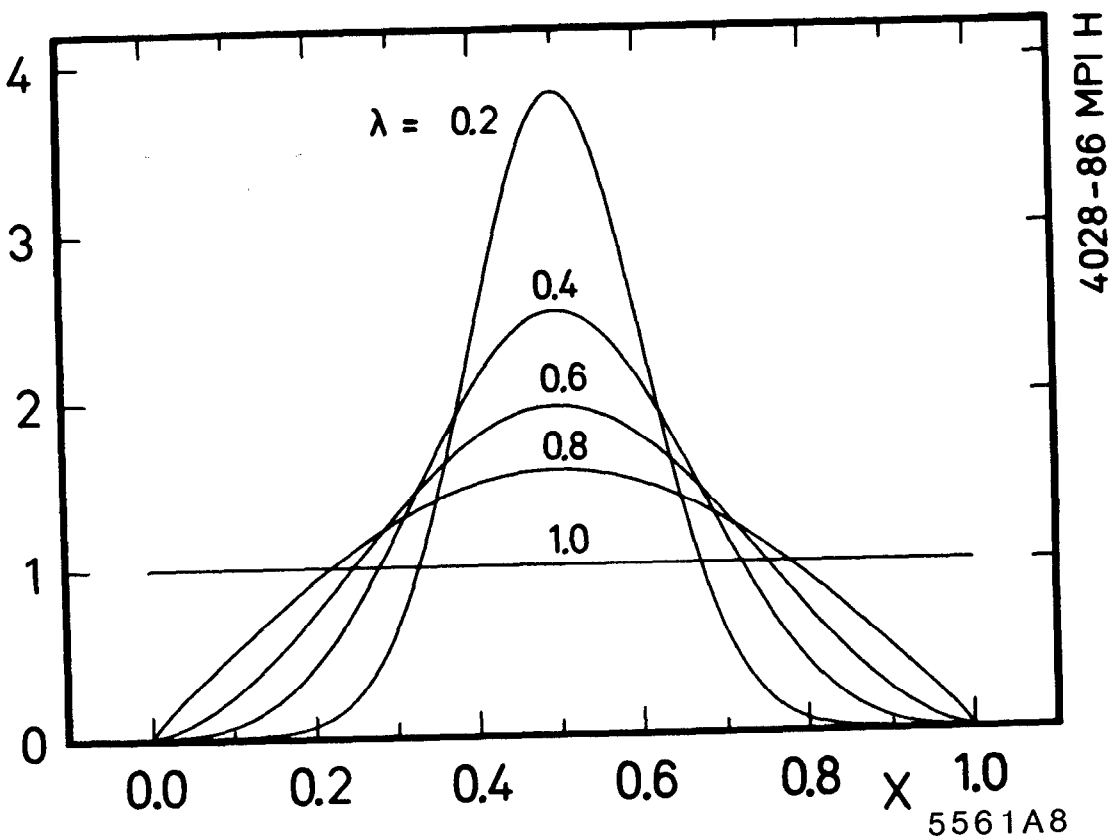

Fig. 8